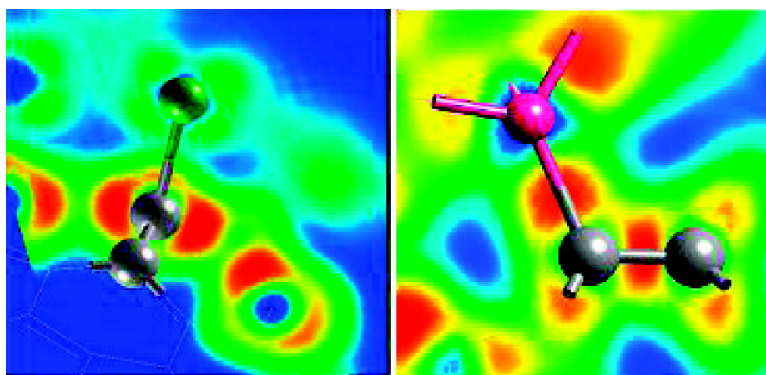


## Metal#Carbon Nanotube Contacts: The Link between Schottky Barrier and Chemical Bonding

Vincenzo Vitale, Alessandro Curioni, and Wanda Andreoni

*J. Am. Chem. Soc.*, **2008**, 130 (18), 5848-5849 • DOI: 10.1021/ja8002843 • Publication Date (Web): 15 April 2008

Downloaded from <http://pubs.acs.org> on February 8, 2009



### More About This Article

Additional resources and features associated with this article are available within the HTML version:

- Supporting Information
- Access to high resolution figures
- Links to articles and content related to this article
- Copyright permission to reproduce figures and/or text from this article

[View the Full Text HTML](#)

## Metal–Carbon Nanotube Contacts: The Link between Schottky Barrier and Chemical Bonding

Vincenzo Vitale, Alessandro Curioni, and Wanda Andreoni\*

IBM Research, Zurich Research Laboratory, 8803 Rüschlikon, Switzerland

Received January 17, 2008; E-mail: and@zurich.ibm.com

The tremendous interest in carbon nanotubes (CNTs) as components of diverse novel devices has spurred extensive research on their physical and chemical properties.<sup>1,2</sup> In particular, the CNT-based field-effect transistor is a promising candidate for the replacement of silicon-based CMOS.<sup>3–5</sup> Since the pioneering work by Heinze et al.,<sup>6</sup> it is common knowledge that charge transport in the CNT channel is controlled by the Schottky barriers that form at the junction with the metal source, and that the nature and geometry of this contact can drastically change the electrical behavior.<sup>7</sup> There is no possibility, however, to obtain information on the structure of the contact from experimental observation. This awareness led to several studies based on computations of various degrees of sophistication<sup>8</sup> aimed at determining the relation between the type of bonding that forms at a given metal contact with a single-wall (SW) CNT and the observed electrical behavior. So far, however, such a correlation has failed to emerge. The side geometry has been almost exclusively investigated, and either small clusters or uniform layers have been used to model the metal along with a graphene sheet to represent the NT or an infinite NT (1D periodic boundary conditions). Moreover, either weak (e.g., ref 8e) or strong (e.g., refs 4, 8a-c) interaction at the metal–CNT junction has been proposed as being the key factor for a “good” contact.

On the basis of extensive *ab initio* calculations performed for both end and side contacts and for two metals of very different nature, namely, Al and Pd, we have found a clear connection between the character of the chemical bonding and the height of the Schottky barrier (SBH). It is the purpose of this Communication to explain how this fundamental link emerges and helps to unravel the combined role of the nature of the metal atoms and of the contact geometry. Our results emphasize that a low SBH for hole conduction in a CNT implies that the  $\pi$ -electron system of the latter is almost exclusively involved in the chemical bonding with the metal atoms at the interface and that the bonding has very specific characteristics in terms of topology and strength. We find that this is the case for Pd in both end and side contacts, but that for Al such an interaction is made possible only by the side configuration. In real systems, Al and Pd provide rather poor and quasi-ideal to ideal transport characteristics, respectively. In particular, estimates of the variation of the SBH as a function of an average value of the tube diameter  $d$  ranging from  $\sim 0.8$  to  $\sim 1.4$  nm (ref 7) indicate a significant difference between metals over the entire range (from  $\sim 0.7$  to  $\sim 0.3$  eV for Al and from  $\sim 0.3$  to 0.0 eV for Pd). Our findings are in agreement with these data and also help to rationalize the behavior of other metals such as Pt.

The present study relies on calculations performed in the framework of density functional theory<sup>9</sup> and a few unprecedented features: atomistic models of relatively large sizes, namely, a (10,0) CNT of length  $\sim 2.5$  nm (11 unit cells) and up to 80 metal atoms distributed either at each end of the tube or around its circumference: Car–Parrinello molecular dynamics for the simulation of the

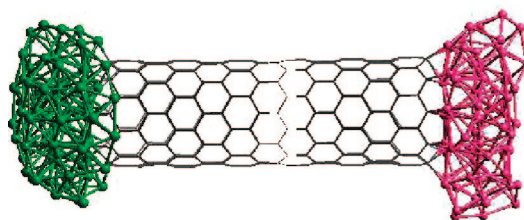


**Figure 1.** Metal–CNT end contacts. Al (right) and Pd (left) shown here on the same graph for the sake of comparison only

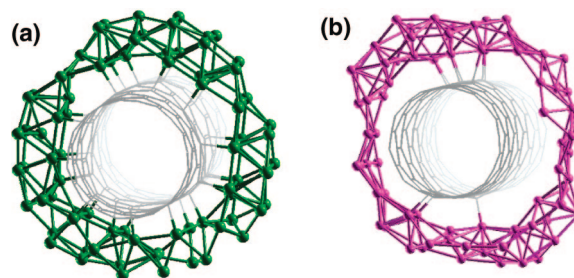


**Figure 2.** Structure of the side contacts. Pd (left) and Al (right).

formation of the metal junction and an analysis of the metal–CNT bonding by means of the electron localization function (ELF)<sup>10</sup> and Bader’s decomposition of the electron density<sup>11</sup> (Bader’s effective atomic charges  $Z_B$ ). Moreover, the search for the optimal geometry was not limited by any constraint, and convergence with the size ( $N$ ) of the metal aggregate was obtained.

Starting from open-end tubes, our Car–Parrinello simulations showed that metal (both Pd and Al) caps form spontaneously (starting from  $N \sim 20$ ) and exhibit an almost regular hexagonal pattern. However, as can be seen in Figure 1, an important difference exists between the two metals: Pd tends to wet the tube, as expected,<sup>4</sup> whereas Al does not. In the side configuration, the higher tendency of Al to coalesce is seen in the much reduced number of bonds,  $N_b$ , it forms with the tube (see Figure 2). Pd atoms, on the other hand, arrange in such a way as to maximize  $N_b$ , which is in agreement with the finding that Pd provides “continuous coating” to suspended SWNTs, while Al does not.<sup>12</sup>

For each case, we calculated the SBH from the “potential profile lineup”,<sup>8b</sup> as reported in Table 1. We note rapid convergence in terms of the size of the metal aggregate, which is consistent with the fact that the origin of the barrier is spatially localized and related to the formation of metal–carbon bonding at the interface. In both end and side configurations, the contact with Pd corresponds to a low SBH, which is in agreement with experiment<sup>7</sup> and all estimates for Pd side contacts (refs 8c,d,f), whereas for Al a very interesting difference is found.

Clarification of these results comes from an inspection of the chemical bonding. ELF plots show that in the “end” geometry a

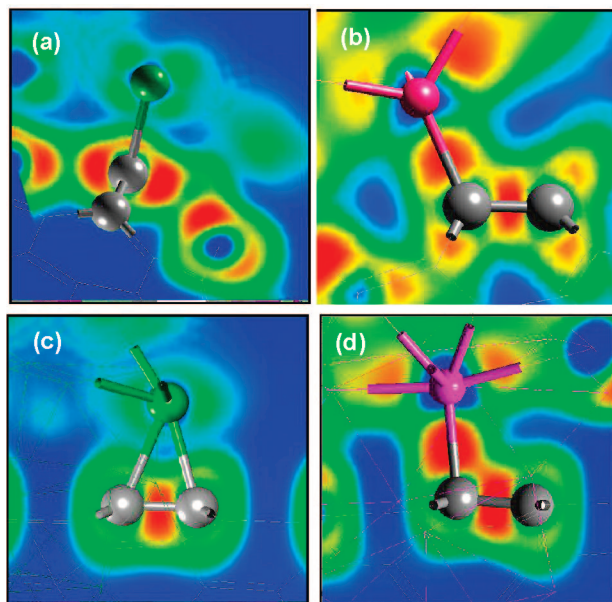


**Figure 3.** ELF at the metal–CNT end (top row) and side (bottom row) contacts for Pd (left) and Al (right).

**Table 1.** Calculated Values of SBHs for Both the End and Side Configurations of the Metal–CNT Contact and for Different Sizes of the Metal Aggregate ( $N$  is the Number of Atoms at Each Contact)

$N$	Pd end	Pd side	Al end	Al side
40	0.07	0.06	0.44	0.12
80	0.07	0.06	0.56	0.13

Pd binds, via a back-donation-like mechanism, to the delocalized CNT  $\pi$ -like system (the Pd–C–C angle is close to  $90^\circ$ , in agreement with an unperturbed  $sp^2$  hybridization of the interacting C atom) (Figure 3a), whereas an Al atom forms a strongly localized  $\sigma$ -bond involving rehybridization of the interacting C toward an  $sp^3$  configuration (the Al–C–C angle is  $\sim 110^\circ$ ), which significantly disturbs the conjugation of the  $\pi$ -like system (Figure 3b). C–Pd bonds are mainly covalent and characterized by a rather limited and delocalized electron transfer from the metal atom ( $\Delta Z_B(\text{Pd}) \sim -0.15$ ), whereas C–Al bonds are strongly localized and correspond to pronounced charge transfer from the metal atom ( $\Delta Z_B(\text{Al})$  up to  $-1.0$ ). The global charge transferred from Pd decays rapidly along the tube with a net flow ( $0.6e$ ) outside the bonded region. No such net flow exists for Al, but slowly decaying charge oscillations stem from the contact, reminiscent of Friedel oscillations at a metal surface. This behavior is consistent with wetting occurring only for Pd (Figure 1). Such a discrepancy can now be associated with the dissimilarity of the interfacial bonding rather than with their relative intrinsic tendency to coalesce, which can be measured in terms of the relative cohesive energies,  $E_c$ . Indeed  $E_c(\text{Al})$  is lower than  $E_c(\text{Pd})$  by  $\sim 15\%$ .<sup>13</sup>

In the side contact, Pd binds to the tube via the same mechanism as in the end configuration, whereas, because of the geometry of the contact and the stable electronic configuration of the C shell, Al interacts with the  $\pi$ -like system, inducing only a limited rehybridization of the interacting C atoms. Correspondingly, the SBH is low also for the Al–CNT contact (Table 1). However, whereas Pd leaves the tube structure essentially unaltered (Figure 2a), there are signs of the tendency of Al to perturb it via strong directional bonds in the induced carbon pyramidalization (Figure

2b). The ELF (Figure 3c,d) confirms this scenario. Also,  $\Delta Z_B(\text{Pd})$  is  $\sim -0.15$ , but  $\Delta Z_B(\text{Al})$  is at most  $-0.5$ .

In conclusion, in addition to the metal work function, the important factor determining the intrinsic SBH was identified as the specific character of the chemical bonding at the interface. A low barrier implies that the coupling of the metal states to those of the CNT essentially takes place with the  $\pi$ -like system and is not too strong so that both orbital hybridization and topology are preserved. This further facilitates the hole transport along the tube. On the other hand, the coupling of the metal states with the  $\sigma$ -like system or, in other words, the perturbation of the conjugation of the  $\pi$ -system via  $sp^3$  C-hybridization is the mechanism enhancing the SBH. In a simple energy-level scheme, one can see this effect, which increases with the interaction strength, as the result of the stabilization of the C p-orbital via rehybridization. This same mechanism is responsible for the observed charge localization and the formation of a dipole at the interface. Thus, the latter has the same origin as the SB and should not be seen as its cause.<sup>8f</sup> Similarly, any structural defect, such as a C-vacancy, will tend to increase the SBH. One can envisage that a supply of energy, for example, through a temperature increase, may also cause Al “to tear” C atoms away from the tube in the side configuration, thus degrading the contact. Finally, a low SBH is a prerequisite for “good contact” once a contact has formed, but this may not occur in real experiments. For example, Pt has a higher work function than Pd and similar SBH can be expected due to the similar bonding characteristics. However its cohesive energy is much higher ( $E_c(\text{Pt}) > E_c(\text{Pd})$  by  $\sim 50\%$ <sup>13</sup>). This can then be seen as the main factor preventing good contact formation.

**Acknowledgment.** Our simulations ran on the BG/L system of the EPFL–Lausanne. We acknowledge the kind hospitality of EPFL and useful discussions with A. Baldereschi and P. Avouris.

**Supporting Information Available:** An image illustrating the behavior of the difference electron density and computational details. This material is available free of charge via the Internet at <http://pubs.acs.org>.

## References

- (1) (a) Dresselhaus, M. S.; Dresselhaus, G.; Avouris, Ph. *Carbon Nanotubes Synthesis, Structure, Properties, and Applications*, Springer: Berlin, Germany, 2001. (b) Bernholc, J.; Brenner, D.; Buongiorno Nardelli, M.; Meunier, V.; Roland, C. *Annu. Rev. Mater. Res.* **2002**, *32*, 347–375. (c) Baughman, R. H.; Zakhidov, A. A.; de Heer, W. A. *Science* **2002**, *297*, 387–392. (d) Burghard, M.; Balasubramanian, K. *Small* **2005**, *1*, 180–192. (e) Avouris, Ph.; Chan, J. *Mater. Today* **2006**, *9*, 46–54.
- (2) Anantram, M. P.; Leonard, F. *Rep. Prog. Phys.* **2006**, *69*, 507–561.
- (3) Avouris, Ph. *Acc. Chem. Res.* **2002**, *35*, 1026–1034.
- (4) Javey, A.; Guo, J.; Wang, Q.; Lundstrom, M.; Dai, H. *Nature* **2003**, *424*, 654–657.
- (5) Klinkke, C.; Hannon, J. B.; Afzali, A.; Avouris, Ph. *Nano Lett.* **2006**, *6*, 906–910.
- (6) Heinze, S.; Tersoff, J.; Martel, L.; Derycke, V.; Appenzeller, J.; Avouris, Ph. *Phys. Rev. Lett.* **2002**, *89*, 106801–106804.
- (7) Chen, Z.; Appenzeller, J.; Knoch, J.; Lin, Y.; Avouris, Ph. *Nano Lett.* **2005**, *5*, 1497–1502.
- (8) (a) Anantram, M. P.; Datta, S.; Xue, Y. *Phys. Rev. B* **2000**, *61*, 14219–14224. (b) Shan, B.; Cho, K. *Phys. Rev. B* **2004**, *70*, 233405–233408. (c) Maiti, A.; Ricca, A. *Chem. Phys. Lett.* **2004**, *395*, 7–11. (d) Zhu, W.; Kaxiras, E. *Nano Lett.* **2006**, *6*, 1415–1418. (e) Nemeč, N.; Tomanek, D.; Cuniberti, G. *Phys. Rev. Lett.* **2006**, *96*, 076802. (f) Zhu, W.; Kaxiras, E. *Appl. Phys. Lett.* **2006**, *89*, 243107–243109.
- (9) Calculations used the CPMD code. Copyright IBM Corp 1990–2008; Copyright MPI für Festkörperforschung Stuttgart, Germany, 1997–2001.
- (10) (a) Becke, A. D.; Edgecombe, K. E. *J. Chem. Phys.* **1990**, *92*, 5397–5403. (b) Savin, A.; Jepsen, O.; Flad, J.; Andersen, O. K.; Preuss, H.; von Schnering, H. G. *Angew. Chem., Int. Ed. Engl.* **1992**, *31*, 187–188.
- (11) Bader, R. F. *Atoms in Molecules: A Quantum Theory*; Oxford University Press: Oxford, 1994.
- (12) Zhang, Y.; Franklin, N. W.; Chen, R. J.; Dai, H. *Chem. Phys. Lett.* **2000**, *331*, 35–41.
- (13) Kittel, C. *Introduction to Solid State Physics* Wiley: New York, 1968.

JA8002843